Fe-binding organic ligands in coastal and frontal regions of the western Antarctic Peninsula

Indah Ardiningsih[1], Kyyas Seyitmuhammedov[2], Sylvia G. Sander[3], Claudine H. Stirling[2], Gert-Jan Reichart[1,4], Kevin R. Arrigo[5], Loes J. A. Gerringa[1], Rob Middag[1,2]

[1]Royal Netherlands Institute for Sea Research (NIOZ), PO Box 59, 1790 AB Den Burg, Department of Ocean Systems, University of Utrecht, the Netherlands
[2]Centre for Trace Element Analysis and Chemistry Department, University of Otago, Dunedin, New Zealand
[3]International Atomic Energy Agency, 4a Quai Antoine 1er, 98000, Principality of Monaco, Monaco
[4]Earth and Geoscience Department, University of Utrecht, Utrecht, the Netherlands
[5]Department of Earth System Science, Stanford University, USA

Correspondence to: Indah Ardiningsih (Indah.ardiningsih@nioz.nl)

Abstract. Organic ligands are a key factor determining the availability of dissolved iron (DFe) in the high nutrient low chlorophyll (HNLC) areas of the Southern Ocean. In this study, organic speciation of Fe is investigated along a natural gradient of the western Antarctic Peninsula, from an ice-covered shelf to the open ocean. An electrochemical approach, competitive ligand exchange - adsorptive cathodic stripping voltammetry (CLE-AdCSV) was applied. Our results indicated that organic ligands in the surface water on the shelf are associated with ice-algal exudates, possibly combined with melting of sea-ice. Organic ligands in the deeper shelf water are supplied via resuspension of slope or shelf sediments. Further offshore, organic ligands are most likely related to the development of phytoplankton blooms in open ocean waters. On the shelf, total ligand concentrations ($[L_t]$) were between 1.2 nM eq. Fe and 6.4 nM eq. Fe. The organic ligands offshore ranged between 1.0 and 3.0 nM eq. Fe. The southern boundary of the Antarctic Circumpolar Current (SB ACC) separated the organic ligands on the shelf from bloom-associated ligands offshore. Overall, organic ligand concentrations always exceeded DFe concentration (excess ligand concentration, $[L']$ = 0.8 - 5.0 nM eq. Fe). The $[L']$ made up to 80% of $[L_t]$, suggesting that any additional Fe input can be stabilized in the dissolved form via organic complexation. The denser modified Circumpolar Deep Water (mCDW) on the shelf showed the highest complexation capacity of Fe ($\alpha_{Fe'L}$; the product of $[L']$ and conditional binding strength of ligands, $K_{Fe'L}^{cond}$). Since Fe is also supplied by shelf sediments and glacial discharge, the high complexation capacity over the shelf can keep Fe dissolved and available for local primary productivity later in the season, upon sea ice melting.

1. Introduction

The Southern Ocean is a High Nutrient Low Chlorophyll (HNLC; e.g. Sunda et al., 1989) region where the phytoplankton biomass is relatively low despite high ambient macronutrient concentrations, i.e. nitrogen (N), phosphorus (P) and silicon (Si) (e.g. Martin et al., 1991; Schoffman et al., 2016). The generally limited availability of light and the micronutrient iron (Fe) prevents phytoplankton from depleting P and N in the vast majority of HNLC areas (de Baar et al., 2005; de Baar, 1990; Martin et al., 1991; Viljoen et al., 2018). Indeed, Fe regulates the dynamics of primary production as it is involved in various cellular processes (Schoffman et al., 2016; Sunda, 1989). In the HNLC Southern Ocean, the availability of Fe has a direct impact on the early spring phytoplankton bloom, and thus on primary productivity (Moore et al., 2013). The Fe limitation in the Southern Ocean could thus have a direct effect on the amount of atmospheric CO_2 sequestration (Le Quéré et al., 2016; Arrigo et al., 2008; Raven and Falkowski, 1999) to the deep ocean via the biological pump (De La Rocha, 2006; Lam et al., 2011). Accordingly, the availability of Fe in the Southern Ocean is not only important for sustaining the food web, but also has a substantial impact on global climate (Henley et al., 2019 and references therein).

The low solubility of Fe in seawater, coupled with low atmospheric and terrestrial input of Fe, result in the scarcity of dissolved-Fe (DFe) in the Southern Ocean. In oxygenated seawater, Fe is mainly present in its oxidized form, Fe(III), predominantly as Fe(III)oxy-hydroxide species. These species tend to undergo further hydrolysis (Liu and Millero, 2002) and are thereby removed from the water column by scavenging or precipitation processes. Organic Fe-binding ligands greatly elevate Fe solubility in seawater (Kuma et al., 1996) by stabilizing Fe in Fe-ligand complexes, and thus allowing Fe to remain longer in the water column. Moreover, Fe bound to organic ligands appears to be bioavailable to marine phytoplankton (Maldonado et al., 2005; Rijkenberg et al., 2008; Hassler et al., 2020). As such, organic ligands are a key component of Fe chemistry and bioavailability, notably in HNLC regions, as illustrated by Lauderdale et al. (2020). These authors showed, with an idealized biogeochemical model of the ocean, that the interaction between microbial ligand production and binding of Fe by these ligands functions as a positive feedback to maintain the DFe standing stock in the oceans.

Different ligand types exist with characteristics (*i.e* binding strength) that are probably related to their origin. The characteristics of organic ligands can be measured by the competition against well-characterized artificial ligands with known stability constants. Analysis is done using an electrochemical technique, competitive ligand exchange (CLE) - adsorptive cathodic stripping voltammetry (AdCSV). The application of AdCSV gives the total concentration ($[L_t]$) and conditional binding strength ($K_{Fe'L}^{cond}$) of the dissolved organic ligands but does not provide information on the identity of ligands. Even though the exact compositions and origins of Fe-binding ligands are

still largely unknown, [L$_t$] and $K_{Fe'L}^{cond}$ obtained by CLE-AdCSV, together with ancillary data, can be used to infer potential sources of these organic ligands. The organic ligands in seawater either have a terrestrial or marine source. The terrestrial-sourced ligands are supplied from lithogenic and pedogenic inputs found within the boundary region between land and sea (*i.e.,* coastal seas and estuaries) (Buck and Bruland, 2007; Batchelli et al., 2010; Kondo et al., 2007; Buck et al., 2007; Bundy et al., 2015; Gerringa et al., 2007; Laglera and van den Berg, 2009).

The marine organic ligands come from *in situ* biological activities, being either actively produced or passively generated through microbial activity. Laboratory studies have documented the active production of Fe-binging ligands under Fe-limited conditions (Boiteau et al., 2013; Boiteau et al., 2016; Butler, 2005). Several types of siderophores, low-molecular-weight organic compounds which have strong affinity to Fe, are produced by mixed marine bacteria communities under Fe stress (Butler, 2005), suggesting that high ligand concentrations are related to a mechanism of Fe acquisition in an Fe-limited environment. These compounds have also been extracted (Boiteau et al., 2016; Macrellis et al., 2001; Velasquez et al., 2011) or identified (Mawji et al., 2008; Velasquez et al., 2016) in field samples. However, they generally occur at picomolar levels (Boiteau et al., 2019) and are a small contributor to the total ligand pool. Other ligand types, such as polysaccharide compounds, are passively generated in situ from microbial excretion and grazing (Sato et al., 2007; Laglera et al., 2019b). The polysaccharides, such as exo-polymeric substances (EPS), are excreted abundantly by a large number of microbial cells, especially in surface water covered by sea-ice (Norman et al., 2015; Lannuzel et al., 2015). Although EPS are relatively labile macromolecules, they can be present in up to micromolar concentrations in seawater, showing the potential to outcompete stronger binding siderophores (Hassler et al., 2017). In addition, humic or humic-like substances (HS) from various origins constitute another type of ligand (Krachler et al., 2015; Laglera et al., 2019a; Whitby et al., 2020). Typically, HS are derived from remineralization and degradation of organic matter (Burkhardt et al., 2014). Terrestrial input of organic matter can supply HS to estuarine and coastal areas, whereas sediment resuspension and upwelling often supply HS to the continental shelf (Gerringa et al., 2008; Buck et al., 2017). HS have also shown to be part of Fe binding ligands in biologically refractory deep ocean dissolved organic matter (rDOM) with low Fe-bioavailability. However, photodegradation of rDOM was shown to increase the Fe bioavailability making Fe bound to such substances an important source in HNLC areas where upwelling plays a role (Hassler et al., 2020; Lauderdale et al., 2020; Whitby et al., 2020; Laglera et al., 2019a).

The Bellingshausen Sea along the western Antarctic Peninsula (WAP) region has a distinct natural DFe gradient (Sherrell et al., 2018; Moffat and Meredith, 2018). The hydrography is strongly influenced by the dynamics of shelf-ocean water exchange. The shoreward intrusion of Circumpolar Deep Water (CDW) provides

macronutrients to the shelf region, whereas offshore-flowing waters supply the micronutrients Fe and Mn to the open ocean from local sources (De Jong et al., 2015; Sherrell et al., 2018), such as glacial meltwater, sediments, and upwelling. The shelf sea of the WAP is a biologically-rich marine ecosystem in the Southern Ocean. The abundance, community composition and trophic structure of marine primary producers are directly impacted by the changing ice conditions and longer periods of open water due to climate change (Turner et al., 2013). Moreover, rapid increases in anthropogenic CO_2 has enhanced the air-sea CO_2 fluxes, decreasing the bulk seawater pH, resulting in ocean acidification (Mikaloff Fletcher et al., 2006), which alters the physicochemical properties of seawater and impacts the organic complexation of Fe (Ye et al., 2020). As the WAP has undergone significant warming (Turner et al., 2020), the changes in ice conditions will influence the supply of Fe and organic ligands, shaping the net primary production in this region. Understanding the sources and distribution of organic ligands provides important information on DFe availability, which is a fundamental step towards understanding the impact of warming of the Antarctic region on primary productivity in the Southern Ocean.

In this study, surface waters were sampled in a region of mixing between shelf-influenced waters and HNLC waters in the Bellingshausen Sea along the WAP. The CLE-AdCSV technique was used to quantify the total concentrations and conditional stability constants of Fe-binding ligands. These parameters were used to examine the distribution of the organic ligands, and to assess their potential sources and influence on the mobilization of Fe in a transect from ice covered shelf waters to the open ocean of the Antarctic Zone.

2. Material and methods

2.1 Sample collection

Samples were collected onboard the research vessel Nathaniel B. Palmer (Cruise NBP1409) during the austral spring between 31 October and 21 November 2014 in the Bellingshausen Sea (Arrigo et al., 2017), west of the Antarctic Peninsula (Figure 1). Water samples were obtained from the surface to maximum 600 m depth at five stations along a transect extending from Adelaide Island on the shelf out into the Bellingshausen Sea in a northwest direction (Figure 1). St. A (70) and B (72) are situated near the shore in the shelf sea, St. C (96) is located at the continental shelf break, and St. D (84) and E (90) are located offshore over deep waters. These stations are a subset of those occupied during the cruise. Hereafter, for simplicity the alphabetical scheme of station numbers will be used, where station A is closest to the coast and station E is furthest from the coast.

Hydrographic parameters were measured using a conventional conductivity-temperature-depth (CTD) rosette equipped with a fluorometer (WET Labs ECOAFL/FL) and an oxygen sensor (SBE-43). Seawater samples for

DFe and Fe-binding ligands in this study were obtained using 12 L GO-FLO bottles attached to a Kevlar® wire.
Seawater samples were filtered over 0.2 µm filters (cellulose acetate, Sartoban 300, Sartorius®) into pre-cleaned sample bottles inside a trace metal clean van. Sample bottles were pre-cleaned following a three-step cleaning protocol for trace element sample bottles (Middag et al., 2009).

Filtered seawater samples for Fe-binding ligand analysis were collected into acid-cleaned 500 mL low density polyethylene (LDPE, Nalgene) bottles and stored at -20°C immediately after collection. For DFe analysis, filtered seawater was collected into acid-cleaned 60 mL LDPE (Nalgene), and acidified to a pH of 1.8 with concentrated quartz-distilled hydrochloric acid (HCl) to give a final concentration of 0.024 M HCl. Filtered samples for macronutrient concentration analysis were stored at -20°C (for N samples) and at 4°C (for Si samples).

2.2
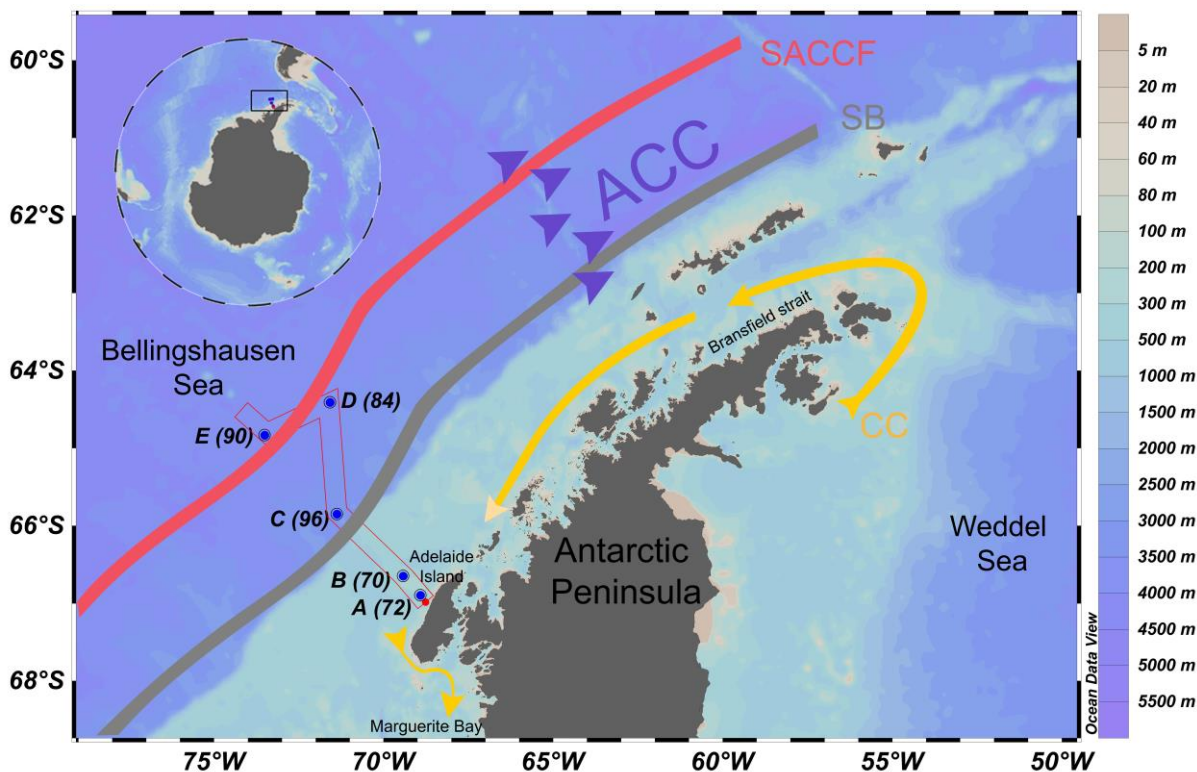
Figure 1: Map of the sampling sites along our study transect near the Western Antarctic Peninsula. The stations are indicated by blue dots and station numbers. The Antarctic Circumpolar Current (ACC) is indicated by purple arrows. The Coastal Current (CC) is indicated by a yellow arrow. The Southern Boundary (SB) of ACC Front is indicated by the grey line. The southern ACC front (SACCF) is

indicated by the red line. See Figure 6 in Arrigo et al. (2017) for details on the ACC flow path. Analysis of DFe and nutrients

The DFe analysis is described in detail by Seyitmuhammedov et al. (in review). In short, the DFe analysis was conducted using high-resolution inductively coupled plasma mass spectrometry (HR-ICP-MS) using a Thermo Fisher Element XR instrument at NIOZ, the Netherlands and using an Amtek Nu Attom instrument at University of Otago, New Zealand. Samples were UV radiated and pre-concentrated using an automated seaFAST system (SC-4 DX seaFAST pico; ESI) equipped with Nobias-PA1 chelate resin. The quantification was done via standard additions to low trace metal seawater. The recovery of the resin was ~100% and was verified in every analytical run by comparison between the slope of the seawater calibration curve and an eluent acid calibration curve after (Biller and Bruland, 2012). Accuracy and reproducibility were monitored by regular measurements of the reference materials SAFe D1 and GEOTRACES South Pacific (GSP) seawater, and an in-house reference seawater sample, North Atlantic Deep Water (NADW). Results for DFe analyses of reference samples were 0.72 $\pm$ 0.01 nM (n = 3; NIOZ) and 0.73 $\pm$ 0.02 nM (n = 6; U. Otago) for SAFe D1 2013 (May 2013 consensus value = 0.69 $\pm$ 0.04 nM) and 0.15 $\pm$ 0.01 nM (n = 13; NIOZ) for GSP 2019 (consensus value = 0.16 $\pm$ 0.045 nM). The average overall method blank (seaFAST and ICP-MS), determined by repeatedly measuring acidified ultrapure water in every analytical run as a sample, was 0.05 $\pm$ 0.02 nM (n = 21). The limit of detection was 0.05 nM, obtained as three times standard deviation of the blank.

2.3 Macronutrients (N and Si) were analyzed simultaneously with a discrete autoanalyzer TRAACS 800 (Technicon) in the shore-based laboratory at NIOZ. Analysis of Fe-binding ligands

Samples were thawed in the dark and vigorously shaken prior to further treatment. Electrochemical analysis CLE-AdCSV with salicylaldoxime (SA) as a competing added ligand (Abualhaija and van den Berg, 2014) was used. In short, the voltammetric system consisted of a BioAnalytical System (BASi) controlled growth mercury electrode connected to an Epsilon 2 analyzer (BASi). The voltammetric system was controlled using ECDsoft interface software. The electrodes in the voltammetric stand included a standard Hg drop working electrode, a platinum wire counter electrode, and a double-junction Ag/AgCl reference electrode (3M KCl).

For the titration, 10 mL sample aliquots were added to 12 pre-conditioned Teflon (Fluorinated Ethylene Propylene (FEP), Savillex) vials and buffered to seawater a pH of 8.2 with 0.1 M ammonium-borate buffer. The sample aliquots were titrated with Fe from 0 to 10 nM (with a 0.5 nM interval from 0 to 3 nM; and with a 2 nM interval from 4 to 10 nM Fe) and vials without Fe addition were prepared twice. Then, the competing ligand, SA, was added at a final concentration of 5 µM. The mixture was left to equilibrate for at least 8 hours or typically overnight

(Abualhaija and van den Berg, 2014). Before analysis, the Teflon vials for titration were pre-conditioned at least three times with seawater containing SA and the intended Fe addition. For each titration point, duplicate scans were done in the same Teflon vial as voltammetric cell.

2.4 Calculation of Fe speciation

Ligand parameters, $[L_t]$ and $K_{Fe'L}^{cond}$, were obtained by fitting the data from the CLE-AdCSV titration into a non-linear Langmuir model. One- and a two-ligand models were applied, assuming one ligand and two ligand groups existed, respectively. The R software package was used for data fitting (Gerringa et al., 2014). The $[L_t]$ reported in nM eq. Fe and the conditional stability constant values are reported as log $K_{Fe'L}^{cond}$.

The values of $[L_t]$, log $K_{Fe'L}^{cond}$, and DFe were used to calculate the concentration of natural unbound ligands, the excess ligands concentration $[L']$, and the side reaction coefficient of ligands ($\alpha_{Fe'L}$; the product of $[L']$ and $K_{Fe'L}^{cond}$, Gledhill and Gerringa (2017). The prime symbol (′) in excess ligand concentrations denotes the free ligands not bound to Fe, whereas the prime symbol after Fe denotes the inorganic fraction of Fe. The value of $\alpha_{Fe'L}$ is presented as a logarithmic value (log $\alpha_{Fe'L}$) and referred to as complexation capacity.

The value of the inorganic Fe side reaction coefficient ($\alpha_{Fe'}$) was determined using the hydrolysis constants of Liu and Millero (1999) at S=36 and at pH of the analysis (pH=8.2). Hence, the value of log $\alpha_{Fe-inorganic}$ =10.4 was used in the calculation for Fe speciation. The conditional stability constant of SA (log $K_{Fe'(SA)}^{cond}$ = 5.94) used in this study is based on the calibration of SA against diethylenetriaminepentaacetic acid by Gerringa et al., (submitted).

3. Results

3.1 Hydrography

Water masses were identified by plotting the Conservative Temperature (Θ) versus the Absolute Salinity (S_A) (Tomczak and Godfrey, 2003) as generated by the freeware ODV (Schlitzer, 2018) from CTD data (Figure 2a). The water mass description follows the definitions of Klinck et al. (2004) and Smith et al. (1999). A detailed description of hydrographic features of the WAP was described elsewhere (Moffat and Meredith, 2018; Klinck et al., 2004; Smith et al., 1999) and briefly summarized here.

Two distinct horizontal currents exist in the study area: the Coastal Current (CC) and the Antarctic Circumpolar Current (ACC) (Figure 1). In the vicinity of the WAP, the ACC is a large strong eastward flowing current

190   bordering the outer continental shelf. The CC is a strong but narrow south-westerly flowing current that is forced

by freshwater discharge and wind over the shelf (Grotov et al., 1998; Moffat and Meredith, 2018). The CC flows

along the coast of the WAP from Bransfield Strait to Marguerite Bay (Figure 1). Our sampling stations are located

along a transect that is perpendicular to the prevailing currents. A number of oceanographic fronts exist along the

ACC (Orsi et al., 1995). Two fronts intersect our sampling transect, namely the southern ACC Front and the

195   southern boundary (SB) of the ACC. These two fronts are present oceanward from the shelf (Figure 1), usually

about 50 – 200 km apart. Although their positions vary, these fronts remain approximately parallel with the

continental shelf break along the WAP (Moffat and Meredith, 2018).
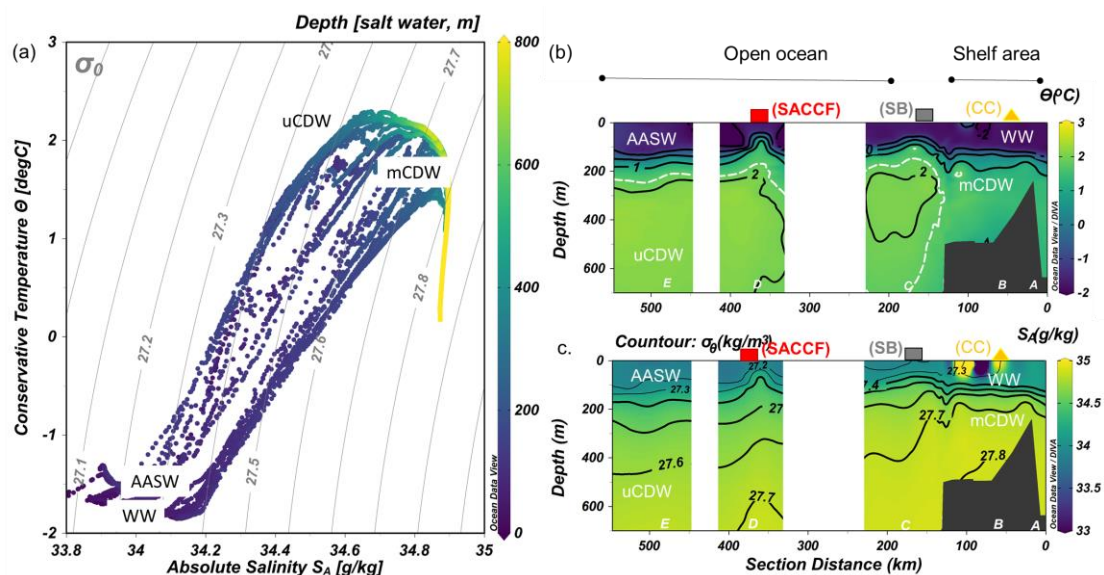
Figure 2: (a) Diagram of absolute salinity (S_A) versus conservative temperature (Θ) with isopycnal lines and colors
200   **denoting depth in m. The distribution along the transect shown in Figure 1 of (b) Θ and (c) S_A with density (σ_θ) as**
contours. The approximate boundary between uCDW and mCDW is marked with a white-dashed line in Figure 2b.
The values of Θ and S_A were generated by ODV software from CTD data.

During the austral spring sampling period, Winter Water (WW; $\Theta < -1.8$ °C and $S_A \sim 34.1$) still existed in the upper

100 m at stations in the shelf sea (Figures 2b and 2c). In spring, Antarctic Surface Water (AASW) forms that has

205   a higher temperature ($-1.5 – 1$°C) and a lower salinity ($33.0 < S_A < 33.7$) than WW (Tomczak and Godfrey, 2003;

Orsi et al., 1995). During sampling, AASW was present at stations outside the shelf region (St. D, E and C; Figures

2b and 2c). The position of the SB marks the southern terminus of water with CDW properties. From the shelf

break toward the open ocean, upper Circumpolar Deep Water (uCDW) existed at 300 m depth, characterized by

$\Theta_{max} = 2$°C and a maximum of $S_A \sim 34.7$. Near the WAP, the Antarctic Slope Front is missing (Klinck et al., 2004;

210   Moffat and Meredith, 2018); hence, there is no barrier in the outer shelf region (Klinck et al., 2004). As a consequence, the shelf region is directly affected by the presence of the SB, resulting in subsurface intrusion of uCDW onto the continental shelf. This water mass is modified into cooler and less saline water, referred to as modified CDW (mCDW) (Hofmann and Klinck, 1998), and was present at stations 70 and 72 below 200 m. Ocean eddies, modulated by wind forcing and interaction with the slope, are responsible for the transport of uCDW from

215   the ACC into the inner shelf region. Intrusion of uCDW displaces shelf water, allowing a heat flux to the shelf area that triggers the melting of floating ice shelves. Melting of the glacial ice produces buoyant northward (offshore) flowing surface water that maintains the continuation of offshore-onshore water mass exchange (Klinck et al., 2004; Moffat and Meredith, 2018), although it did not seem to occur along our transect.

    The ice-coverage diminished with increasing distance from the shore, with stations near-shore (St. A and B)

220   having sea ice concentrations of 100%, and falling to 60% at the shelf break (St. C). The ice-cover dropped to 20% at St. D offshore, whereas St. E was ice free.

3.2 Fe speciation

    Stations located in the continental shelf (St. A and B) generally had higher $[L_t]$ and DFe than stations sampled offshore (St. C, D and E; Figures 3a and 3b). At the shelf stations, $[L_t]$ varied from 1.23 to 6.43 nM eq. Fe and

225   high $[L_t]$ (>2 nM) was present below 200 m in mCDW (Figure 3a). In particular, at St. A nearest to the shore, $[L_t]$ was higher than 2.5 nM eq. Fe at the surface and reached up to 6.43 nM eq. Fe at 400 m close to the sediment. Concentrations of DFe were <0.6 nM (0.29 - 0.52 nM) in the upper 100 m, but >1 nM (1.11 to 2.26 nM) at depths below 200 m near the sediment (Figure 3b).
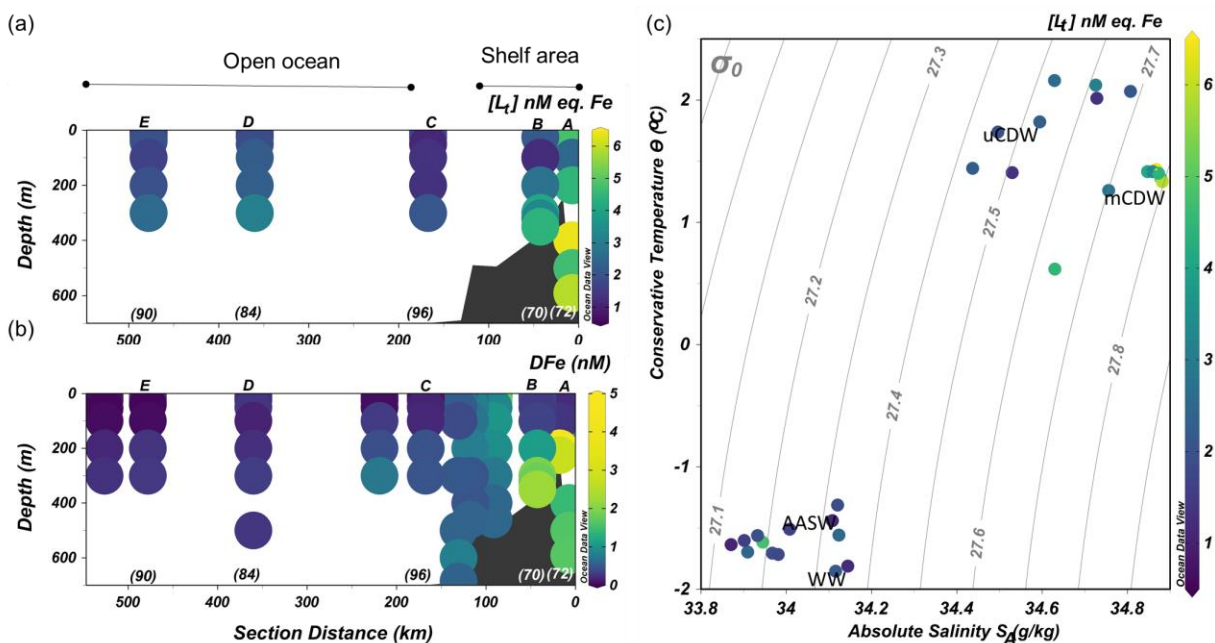
Figure 3: The distribution along the transect shown in Figure 1 of (a) the concentrations of total Fe-binding ligand [L_t] and (b) concentrations of dissolved-Fe (DFe, data from Seyitmuhammedov et al., (in review); and (c) a Θ-S_A diagram with colors denoting the values of [L_t]. The letters above and numbers below the profiles in (a) and (b) indicate the stations. DFe data are presented using a non-linear scale for clarity.

Further offshore towards the open ocean (St. C, D and E), [L_t] varied from 1.07 to 3.09 nM eq. Fe (Figure 3a), whereas DFe concentrations ranged from <0.05 and 0.47 nM (Figure 3b). At the shelf break, approximately where the SB was located, [L_t] was relatively low (St. C; Figure 3a). Low DFe was observed in the upper 200 m offshore, reaching the lowest concentration (<0.05 nM) at St. E farthest from the shelf (Figure 3b).

Two ligand groups were distinguished only in two samples in open ocean waters, both collected at St. E (at 40 and 300 m). The measured conditional stability constant for the stronger L_1 ligands and the progressively weaker L_2 ligands were distinct, and the values did not overlap. At 40 m, $\log K_1 = 12.4\pm1.1$ and $\log K_2 = 10\pm1.1$, whereas at 300 m, $\log K_1 = 11.3\pm0.6$ and $\log K_2 =10.4\pm0.7$. However, the uncertainty for the ligand concentrations was relatively large for the two-ligand model, L_1 (0.66±1.81 and 1.58±4.29 nM eq. Fe, at 40 and 300 m, respectively) and L_2 (1.10±4.32 and 1.34±3.74 nM eq. Fe, at 40 and 300 m, respectively), which implies that the one-ligand model fit the data better. Therefore, results of data fitting with the two-ligand model will not be presented.
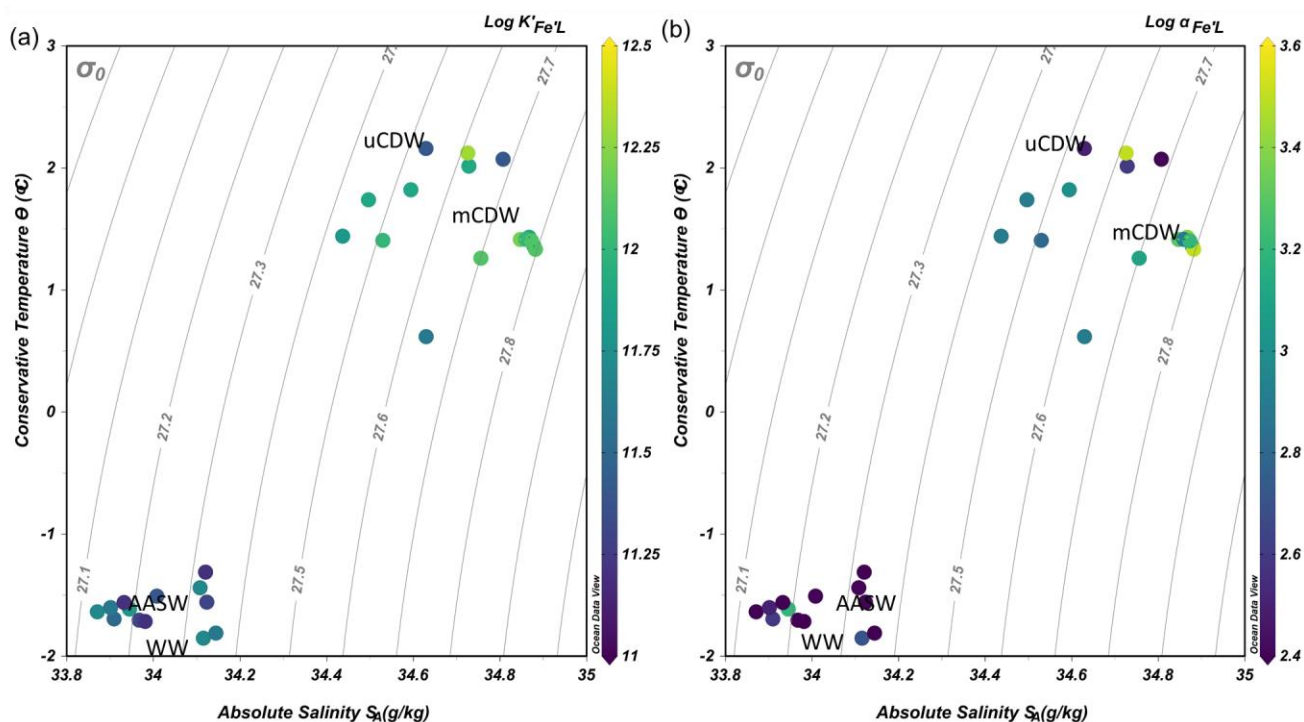
245

Figure 4: (a) The binding strength, log $K_{Fe'L}^{cond}$ and (b) complexation capacity, log $\alpha_{Fe'L}$ plotted in a Θ-S_A diagram. The color scale indicates the values of log $K_{Fe'L}^{cond}$ and log $\alpha_{Fe'L}$.

The values of log $K_{Fe'L}^{cond}$ varied within one order of magnitude between 11.1 and 12.3 (Figure 4a). The lower log $K_{Fe'L}^{cond}$ in AASW coincided with the lowest log $\alpha_{Fe'L}$ (AASW: mean log $\alpha_{Fe'L}$ = 2.6±0.3, N=13; Figure 4b). The

250 largest log $K_{Fe'L}^{cond}$ and log $\alpha_{Fe'L}$ was measured in shelf waters, particularly in mCDW (mean log $\alpha_{Fe'L}$ =3.4±0.2, N=8; Figure 4b). Overall, a decreasing trend of log $K_{Fe'L}^{cond}$ and log $\alpha_{Fe'}$ was observed in mCDW, uCDW and AASW with highest values in mCDW and lowest in AASW.

Ligands were always present in excess of DFe, with [L′] ranging from 0.75 to 4.98 nM eq. Fe. High excess ligand concentrations (>2 nM eq. Fe) were observed close to shore (St. A) declining towards the shelf break and reaching

255 the lowest [L′] at St. C near the shelf break (Figure 5a). Further offshore (St. D and E), [L′] remains fairly constant at 1 – 2 nM eq. of Fe.

Figure 5: The distribution along the transect shown in Figure 1 of (a) excess ligand concentrations [L′], (b) Fluorescence, and (c) Nitrate.

4. Discussion

260   The ligand concentrations measured during our study (1.07 – 6.43 nM eq. Fe; Figure 3a) are consistent with the broad range of Fe-binding ligand concentrations measured in DFe speciation studies in the Southern Ocean (Boye et al., 2001; Lin and Twining, 2012; Nolting et al., 1998; Thuróczy et al., 2011). Previously reported [L_t] in the Southern Ocean varies from 0.5 – 1.84 nM eq. Fe in the Atlantic sector (Thuróczy et al., 2011), 2.2 to 12.3 nM eq. Fe in the Pacific sector (Nolting et al., 1998), and 0.44 – 1.61 nM eq. Fe in the Indian sector (Gerringa et al.,

265   2008). The [L_t] in Antarctic polynyas ranges between 0.3 – 1.6 nM eq. Fe (Gerringa et al., 2019; Thuróczy et al., 2012), whereas in regions with sea ice-coverage, [L_t] in underlying water is relatively high, with values of 4.9 – 9.6 nM eq. Fe and up to 72.1 nM eq. Fe within the sea ice (Lannuzel et al., 2015; Genovese et al., 2018).

4.1 Fe-binding ligands along the transect from the shelf to the open ocean

The high sea ice cover on the continental shelf obstructs the light penetration into the water column, inhibiting the

270   development of an early spring bloom. Therefore, bloom generated ligands are less likely to be found. However, microbial excretion from sea-ice algae and bacteria within and just beneath the sea-ice release EPS, which can form Fe-binding ligands (Lannuzel et al., 2015; Norman et al., 2015; Genovese et al., 2018; Hassler et al., 2017). The planktonic community in spring is dominated by diatoms and haptophytes (*Phaeocystis antarctica*) (Joy-Warren et al., 2019; Arrigo et al., 2017). According to Lannuzel et al. (2015), the omnipresence of tube dwelling

275   diatoms (*Berkelaya* sp.) attached via EPS to the bottom of the sea-ice was responsible for relatively high [L_t] in under-ice seawater, indicating that EPS could elevate seawater [L_t] in areas of sea-ice cover. In addition, a laboratory study has shown that cultured *P. antarctica* appears to excrete EPS in relatively high concentrations (Norman et al., 2015), with similar binding strength (log $K_{Fe'L}^{cond}$ 11.5 – 12) to those measured in this study (log $K_{Fe'L}^{cond}$ 11.1 – 12.3). At the ice-covered shelf stations, the high [L_t] in the upper water column implies that ice algae

280   exudates are a source of Fe-binding ligands (St. A and B; Figure 3a). Further from the coast, EPS from phytoplankton likely provide an additional surface source of ligands.

High [L_t] (>2.75 nM eq. Fe) was observed in mCDW (Figure 3c) with a narrow range of log $K_{Fe'L}^{cond}$ (11.1 - 11.9; Figure 4a), which suggests similar chemical characteristics and a common origin. Given that uCDW at the shelf break has [L_t] lower than 2.5 nM eq. Fe and relatively low DFe concentrations, the high [L_t] in mCDW appears

285   to be supplied by the shelf sediments. Upwelling and contact with the sediment of uCDW presumably results in the resuspension of organic matter and pore water from the sediment, supplying ligands and DFe to the water

column. Indeed, ligand input in the proximity of sediments was previously observed in upwelling regions over the continental shelf or in coastal areas (Gerringa et al., 2008; Buck et al., 2017). Subsequent upwelling processes may transport the ligands to the upper water column, including rDOM. Moreover, intrusion of uCDW also provides heat (Smith et al., 1999), which may cause glacial and sea ice melt. The melting of sea ice (i.e. first year pack ice) supplies ligands to surrounding seawater (Genovese et al., 2018), whereas glacial ice is not expected to contribute organic ligands. The estimated flux of [L_t] from melting pack ice in spring can reach up micromolar levels per square meter of pack-ice per day (Genovese et al., 2018), showing the significance of the sea-ice melt contribution to the ligand pool. Overall, the high [L_t] in the shelf region (Figure 3a) can be explained by several ligand sources associated with sea-ice, including the melting of sea-ice, as well as sediment resuspension and upwelling.

At the continental shelf break (St. C) in the vicinity of the SB, the lowest [L_t] was found in the upper 200 m of the water column. The presence of the SB is noticeable by the increased upward tilt of the isopycnals (Figure 2a) (Orsi et al., 1995; Klinck et al., 2004). Here the ACC interacts with the continental slope (Orsi et al., 1995), propagating ocean eddies that subsequently cause cross-shelf water intrusion (Moffat and Meredith, 2018). The subsurface intrusion of uCDW and its associated turbulence may cause vertical water mass mixing at the proximate location of the SB. The little ice-cover at the shelf break compared to the inner shelf allows more light penetration, triggering a bloom, as indicated by a fluorescence maximum observed at St. C (Figure 5b). The bloom and its related microbial activities could release Fe-binding ligands. However, given the consistently low and constant distribution of [L_t] at the shelf break, it seems that mixing determines the distribution and net concentrations of ligands (Figure 3a) and likely the microbial species composition as well. Different microbial species have different rates of organic ligand production, and different microbial species may produce different types of organic ligands (Norman et al., 2015). The influence of mixing on ligands and microbial species composition is confirmed by the relatively constant distribution of DFe and macronutrients (i.e., nitrate; Figure 5c) at the same station, indicating that prominent mixing at the shelf break indeed is a major factor.

Further oceanward from the shelf break, [L_t] was >1 nM eq. of Fe (St. D and E; Figure 3a), probably related to the spring bloom at this location. Satellite-based data (Arrigo et al., 2017), showed that open water formed one month earlier offshore than near-shore (St. A and B), implying that the melting of sea ice offshore (St. D and E) occurred preceding and during our occupation. The melting of sea ice released nutrients and micronutrients such as Fe (Lannuzel et al., 2016; Sherrell et al., 2018), which together with the availability of light stimulated the spring bloom. Such a bloom in turn is a source of Fe-binding ligands in the upper water column (Gledhill and Buck, 2012; Boye et al., 2001; Croot et al., 2004; Gerringa et al., 2019). Arrigo et al. (2017) reported that a bloom

in its early stages was observed underneath variable sea ice cover seaward from the shelf break. Indeed, the fluorescence maxima observed in the upper 100 m at the offshore stations (St. D and E; Figure 5b) concurred with

320   depletion of DFe and drawdown of macronutrients (N and Si), illustrating the presence of a bloom. Siderophores are expected to be produced upon Fe depletion by marine microbes as a strategy to acquire Fe (Butler, 2005; Buck et al., 2010; Mawji et al., 2008; Velasquez et al., 2011). Similarly, as detailed above for the shelf stations, the exudation of EPS from diatoms and haptophytes could be an important addition to the organic ligand pool. Moreover, polysaccharide ligands will be released by microbial cells during the bloom as well as via grazing (Sato

325   et al., 2007; Laglera et al., 2019b) and viral lysis (Poorvin et al., 2011; Slagter et al., 2016). Additionally, the ratios of labile particulate Fe to labile particulate Mn (0.27 ± 0.49 nM; Seyitmuhammedov et al. (in review)) indicate that Fe has a biogenic origin in the offshore waters (Twining et al., 2004). Therefore, we suggest that the origin of $[L_t]$ offshore was, next to the melting of sea ice, the result of *in situ* production of organic ligands during the bloom and passive generation from microbial processes associated with the bloom.

330   The lowest concentrations of DFe (<0.05 nM) were observed at St. D and E and were a result of both biological uptake and limited supply. This area most likely represents Fe-limited conditions as indicated by declining Si* (Si*= [Si] – [N]) values and high ratios of [nitrate]/DFe (Figures 6a and 6b). The value of Si* serves as a proxy for Fe limitation, where Fe stress leads to preferential drawdown of Si compared to N by diatoms in surface water (Takeda, 1998). A negative Si* indicates Fe limiting conditions, assuming that Si and N are required in a 1:1 ratio

335   by diatoms (Brzezinski et al., 2002). In our dataset, although there were no negative values for Si*, some Si* values at the open ocean stations were close to zero. Our data indicate that although there is no Fe-limitation during our sampling period, Fe limitation could potentially develop later in the season. Typically, organic ligands excreted under Fe-limited conditions have strong affinity for Fe (Maldonado et al., 2005; Mawji et al., 2008), i.e. a high log $K_{Fe'L}^{cond}$ (>12). However, a relatively low log $K_{Fe'L}^{cond}$ is observed in AASW relative to deeper uCDW and

340   mCDW (Figure 4a). This indicates that in offshore AASW where Fe limitation is expected, the contribution of siderophores is modest. Indeed, recent studies showed that only <10% of Fe is complexed by siderophores (Boiteau et al., 2019; Bundy et al., 2018), suggesting that the binding strength of the overall ligand pool is not always a good indicator of the presence of particular ligand group if multiple ligand sources are present. Moreover, in the presence of light, organic ligands can undergo photo-degradation(Hassler et al., 2020), and thus the chemical

345   structure can be altered into a slightly weaker ligand type (Barbeau et al., 2001; Powell and Wilson-Finelli, 2003). Mopper et al. (2015) suggested that the absorption of solar radiation by chromophoric dissolved organic matter as part of the ligand pool. These chromophoric compounds are commonly produced by sea ice algae (Norman et

al., 2011), leading to the photochemical transformation of these compounds. These photo-oxidative processes can thus also explain the shift in log $K_{Fe'L}^{cond}$ in the AASW to lower values compared to deeper uCDW and mCDW.
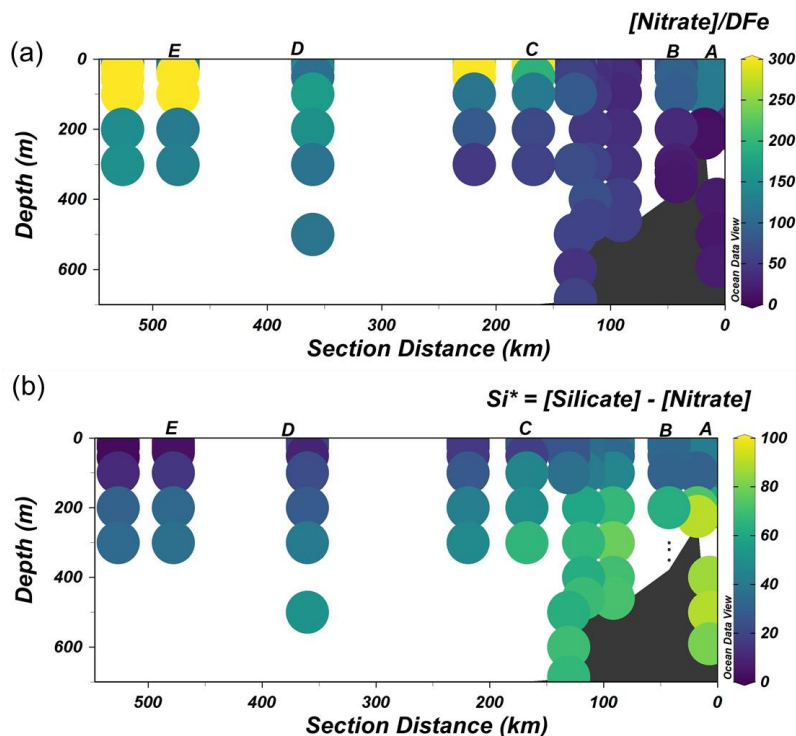
Figure 6: The distribution of Si*(a) and the ratio of [Nitrate]/DFe (b) along the transect shown in Figure 1.

The presence of the SACCF and SB fronts affects bloom conditions. As shown by Arrigo et al. (2017), high chlorophyll-a concentrations were observed in surface waters in between the SB and SACCF, which suggest the distribution of phytoplankton biomass is affected by physical processes in the area. The SB also appears to mark the boundary between offshore organic ligands that result from a combination of the earlier sea ice melt and *in situ* production and/or generation associated with offshore blooms, and organic ligands on the shelf that result from a combination of ice-algae exudation, sea-ice melt, and sediment resuspension. In the region near the SB at the shelf break, water mass mixing due to the baroclinically unstable water column seems to have caused consistent distributions of [L_t] (Figure 3a). Further offshore, ligands are most likely associated with the bloom, but the distribution of ligands is also affected by enhanced vertical mixing and intensified currents proximal to the area of the fronts. Solar radiation enhances stratification and drives the formation of the spring bloom whereas

deep mixing can both hinder as well as stimulate bloom formation based on the balance between availability of light and nutrients (Arrigo et al., 2017). It thus seems likely that the balance between mixing and stratification results in variable [L_t] in the area around the SACCF (St. D and E; Figure 3a).

4.2 Implications for primary productivity

In general, we found [L'] >0.75 nM eq. Fe (Figure 5a), which accounts for approximately 80% of [L_t]. This implies that at least 80% of total ligands measured are available to bind Fe, although the total complexation capacity of ligands is also determined by its log $K_{Fe'L}^{cond}$. The highest complexation capacity log $\alpha_{Fe'L}$ was found in mCDW on the shelf (Figure 4b), and concurred with the highest concentrations of DFe in mCDW (Figure 3b and Figures 4b). The high complexation capacity of ligands on the shelf increases the potential of organic ligands to stabilize additional Fe input to the shelf waters (Lannuzel et al., 2015; Gerringa et al., 2019; Thuróczy et al., 2012) and lengthen the residence time of DFe (Gerringa et al., 2015). A longer residence time has a positive feedback on the development of local primary productivity upon sea ice melting (Arrigo et al., 2017), supplying DFe to primary producers on the shelf, which were dominated by *Phaeocystis antarctica* during our sampling period (Joy-Warren et al., 2019). Moreover, the results of our oxygen isotope ($^{18}O/^{16}O$, conventionally reported into delta-notation as $\delta^{18}O$; Seyitmuhammedov et al. (in review)) analysis showed that $\delta^{18}O$ values ranged from -0.56 – 0.06 ‰. These values were used to estimate fractions of sea-ice meltwater (-1.9 – 1.1 %) and meteoric meltwater (precipitation and glacial; 0.3 – 3.9 %). Based on those results, meltwater associated with runoff and glacial discharge is present in the upper 200 m of the shelf region, and probably is a source of particulate and dissolved Fe that will increase under continued climate change. However, whether Fe in particulate form will partition into the dissolved pool via ligand driven dissolution of Fe, also depends on the fraction of labile particulate Fe. In addition, local primary productivity not only relies on the DFe input from, for example, meltwater and glacial debris (Klunder et al., 2011; Lannuzel et al., 2016), but probably also on the input of Co and Mn (Saito et al., 2010; Wu et al., 2019; Middag et al., 2013) as these elements showed co-limitation in the Southern Ocean (Middag et al., 2013; Saito and Goepfert, 2008).

Besides affecting the shelf conditions, ice melt also produces buoyant northward-flowing surface water, which may facilitate DFe transport from the shelf to the open ocean, supplying DFe for primary production offshore, but this effect was not noticeable in the transport data for this specific transect. However, the conditions along the WAP were not homogenous and elevated Fe (up to 4.88 nM for DFe ; Seyitmuhammedov et al. (in review) concentrations northeast of our transect were observed in the upper 100 m, suggesting that some of the observed ligands might have been transported southwesterly with the CC. This high DFe stabilized by organic ligands will

probably be transported further to the southwest where a coastal polynya is commonly observed in Marguerite Bay (Arrigo et al., 2015). Such transport would supply DFe to the highly productive Marguerite Bay polynya and fuel phytoplankton blooms in these ice-free waters but could also be partly transported offshore in the region southwest of our transect. However, the relative amount of DFe bound to organic ligands can vary, and is also strongly influenced by the continued change in environmental conditions due to global warming (Slagter et al., 2017; Ye et al., 2020), making it likely such a transport of DFe to the southwest or offshore will change as well. Global warming has caused glaciers to retreat and induced significant loss of sea-ice, particularly in the Antarctic Peninsula area (Henley et al., 2019; Stammerjohn et al., 2012; Turner et al., 2020). The sea ice extent over the southern Bellingshausen Sea, has decreased in recent decades, creating open water and lengthening the ice-free season (Turner et al., 2013). This results in increased solar irradiance and enhanced stratification (Henley et al., 2019), which can lead to an alteration of the phytoplankton community structure. As previously reported, variable light conditions favor the growth of *Phaeocystis antarctica* over diatoms (Joy-Warren et al., 2019; Alderkamp et al., 2012). In contrast, smaller-cell diatoms are better adapted to increased sea surface temperature (Schofield et al., 2017). Changes in planktonic community composition affect net primary production and overall carbon drawdown, which lead to further alteration of the food web and carbon cycling (Schofield et al., 2017; Joy-Warren et al., 2019; Arrigo et al., 1999; Alderkamp et al., 2012). These and other ongoing changes in the food web will also affect production of dissolved organic carbon (DOC) and thus ligands as they form a fraction of the DOC pool (Gledhill and Buck, 2012; Whitby et al., 2020). Generally, one expects that increased DOC production would lead to more ligands, but the binding strength depends on which molecules are formed (Gledhill and Buck, 2012; Hassler et al., 2017). Additionally, intensified light exposure alters log $K_{Fe'L}^{cond}$ by photo-oxidative processes, possibly reducing the complexation capacity and binding strength for Fe (Barbeau et al., 2001; Powell and Wilson-Finelli, 2003; Mopper et al., 2015) as well as the bioavailability (Hassler et al., 2020). Furthermore, complexation capacity is affected by pH, implying that ongoing ocean acidification also influences the speciation of Fe (Ye et al., 2020), although the extent to which these changes are important is not yet known. The melting of sea-ice with entrapped sediment, potentially releases organic ligands (Genovese et al., 2018). Additionally, organic ligands from microbial excretions are expected to be abundant at the base of sea ice (Norman et al., 2015). Overall, the continued sea-ice melt and glacial retreat can be expected to increase the supply of Fe (Lannuzel et al., 2016), other micronutrients (Co, Mn, etc.), and Fe-binding ligands (Lin and Twining, 2012), but the consequences for their complexation capacity and overall bio-availability of Fe remain elusive. If DFe becomes progressively more available in the Southern Ocean, phytoplankton growth could increase until another process becomes limiting, such as the availability of another micronutrient or macronutrient. Many uncertainties remain, but the changing

environmental conditions of the WAP due to climate change will affect marine biogeochemical cycles and influence productivity beyond the Southern Ocean as the Southern Ocean is an important hub in ocean circulation and its waters eventually supply nutrients to other regions (e.g. Middag et al., 2020).

5. Summary

Our results indicate that organic Fe-binding ligands in surface water on the continental shelf of the WAP are associated with ice-algal exudates and addition of ligands from melting sea ice. In the water column close to the continental slope and shelf sediments, resuspension of sediment followed by upwelling processes appears to be another source of ligands. From the continental shelf-break oceanward, sources of Fe-binding ligands are likely related to offshore phytoplankton blooms, either actively produced during the bloom, or passively generated by microbial processes associated with the bloom. The distribution of ligands is affected by the two major fronts in the region, the SACCF and SB. The SB along the shelf break not only marks the boundary between the shelf and open ocean, but also marks the border between organic ligands associated with the bloom offshore and organic ligands on the shelf originating from sea-ice and sediment related sources, such as ice-algae exudation, sea-ice melt, and sediment resuspension. Overall, excess ligands comprised up to 80% of the total ligand concentrations, implying the potential to solubilize additional Fe input. The ligands in denser mCDW on the shelf have a higher complexation capacity for Fe, and are thus capable of increasing the residence time of Fe as DFe and fuel local primary production later in the season upon ice melt.

6. Author contribution

IA and KS performed the analysis. IA and LG prepared the content of the manuscript. RM collected the samples, lead the design of this research and edited the manuscript. SS and CS contributed to research design and edited the manuscript. KRA performed the research and edited the manuscript. All authors contributed to the final version of the manuscript.

7. Acknowledgements

The authors would like to thank the captain and his crew of the R/VIB N. B. Palmer, as well as Anne-Carlijn Alderkamp and all other participants, for their efforts and support. Our colleagues in the nutrient lab at NIOZ are acknowledged for analyzing nutrients. IA was financed by Indonesia Endowment Fund for Education (LPDP),

450   and KS received a scholarship from the University of Otago. KRA was funded by a grant from the National Science Foundation Office of Polar Programs (ANT-1063592). The IAEA is grateful to the Government of the Principality of Monaco for the support provided to its Environment Laboratories.

8.   Data availability

Data can be found at https://doi.org/10.25850/nioz/7b.b.5

455   ## 9.   Competing interest

The authors declare that they have no conflict of interest.

10. References

Abualhaija, M. M., and van den Berg, C. M. G.: Chemical speciation of iron in seawater using catalytic cathodic stripping voltammetry with ligand competition against salicylaldoxime, Marine Chemistry, 164, 60-74,
460   10.1016/j.marchem.2014.06.005, 2014.
Alderkamp, A.-C., Kulk, G., Buma, A. G. J., Visser, R. J. W., Van Dijken, G. L., Mills, M. M., and Arrigo, K. R.: The effect of iron limitation on the photophysiology of phaeocystis antarctica (prymnesiophyceae) and fragilariopsis cylindrus (bacillariophyceae) under dynamic irradiance, Journal of Phycology, 48, 45-59, 10.1111/j.1529-8817.2011.01098.x, 2012.
465   Arrigo, K. R., Robinson, D. H., Worthen, D. L., Dunbar, R. B., DiTullio, G. R., VanWoert, M., and Lizotte, M. P.: Phytoplankton Community Structure and the Drawdown of Nutrients and CO2 in the Southern Ocean, Science, 283, 365-367, 10.1126/science.283.5400.365, 1999.
Arrigo, K. R., van Dijken, G., and Long, M.: Coastal Southern Ocean: A strong anthropogenic CO2 sink, Geophysical Research Letters, 35, 0094-8276, 10.1029/2008GL035624, 2008.
470   Arrigo, K. R., van Dijken, G. L., and Strong, A. L.: Environmental controls of marine productivity hot spots around Antarctica, Journal of Geophysical Research: Oceans, 120, 5545-5565, 10.1002/2015JC010888, 2015.
Arrigo, K. R., van Dijken, G. L., Alderkamp, A.-C., Erickson, Z. K., Lewis, K. M., Lowry, K. E., Joy-Warren, H. L., Middag, R., Nash-Arrigo, J. E., Selz, V., and van de Poll, W.: Early Spring Phytoplankton Dynamics
475   in the Western Antarctic Peninsula, Journal of Geophysical Research: Oceans, 122, 9350-9369, 10.1002/2017jc013281, 2017.
Barbeau, K., Rue, E. L., Bruland, K. W., and Butler, A.: Photochemical cycling of iron in the surface ocean mediated by microbial iron(iii)-binding ligands, Nature, 413, 409-413, 10.1038/35096545, 2001.
Biller, D. V., and Bruland, K. W.: Analysis of Mn, Fe, Co, Ni, Cu, Zn, Cd, and Pb in seawater using the Nobias-
480   chelate PA1 resin and magnetic sector inductively coupled plasma mass spectrometry (ICP-MS), Marine Chemistry, 130, 12-20, 10.1016/j.marchem.2011.12.001, 2012.

Boiteau, R. M., Fitzsimmons, J. N., Repeta, D. J., and Boyle, E. A.: Detection of iron ligands in seawater and marine cyanobacteria cultures by high-performance liquid chromatography-inductively coupled plasma-mass spectrometry, Analytical Chemistry, 85, 4357-4362, 10.1021/ac3034568, 2013.

485 Boiteau, R. M., Mende, D. R., Hawco, N. J., McIlvin, M. R., Fitzsimmons, J. N., Saito, M. A., Sedwick, P. N., DeLong, E. F., and Repeta, D. J.: Siderophore-based microbial adaptations to iron scarcity across the eastern Pacific Ocean, Proceedings of the National Academy of Sciences of the United States of America, 113, 14237-14242, 10.1073/pnas.1608594113, 2016.

Boiteau, R. M., Till, C. P., Coale, T. H., Fitzsimmons, J. N., Bruland, K. W., and Repeta, D. J.: Patterns of iron
490 and siderophore distributions across the California Current System, 64, 376-389, doi:10.1002/lno.11046, 2019.

Boye, M., van den Berg, C. M. G., de Jong, J. T. M., Leach, H., Croot, P., and de Baar, H. J. W.: Organic complexation of iron in the Southern Ocean, Deep-Sea Research Part I-Oceanographic Research Papers, 48, 1477-1497, 10.1016/s0967-0637(00)00099-6, 2001.

495 Brzezinski, M. A., Pride, C. J., Franck, V. M., Sigman, D. M., Sarmiento, J. L., Matsumoto, K., Gruber, N., Rau, G. H., and Coale, K. H.: A switch from $Si(OH)_4$ to NO_3^- depletion in the glacial Southern Ocean, Geophysical Research Letters, 29, 5-1-5-4, 10.1029/2001gl014349, 2002.

Buck, K. N., Selph, K. E., and Barbeau, K. A.: Iron-binding ligand production and copper speciation in an incubation experiment of Antarctic Peninsula shelf waters from the Bransfield Strait, Southern Ocean,
500 Marine Chemistry, 122, 148-159, 10.1016/j.marchem.2010.06.002, 2010.

Buck, K. N., Sedwick, P. N., Sohst, B., and Carlson, C. A.: Organic complexation of iron in the eastern tropical South Pacific: Results from US GEOTRACES Eastern Pacific Zonal Transect (GEOTRACES cruise GP16), Marine Chemistry, 10.1016/j.marchem.2017.11.007, 2017.

Bundy, R. M., Boiteau, R. M., McLean, C., Turk-Kubo, K. A., McIlvin, M. R., Saito, M. A., Van Mooy, B. A. S.,
505 and Repeta, D. J.: Distinct Siderophores Contribute to Iron Cycling in the Mesopelagic at Station ALOHA, Frontiers in Marine Science, 5, 10.3389/fmars.2018.00061, 2018.

Burkhardt, B. G., Watkins-Brandt, K. S., Defforey, D., Paytan, A., and White, A. E.: Remineralization of phytoplankton-derived organic matter by natural populations of heterotrophic bacteria, Marine Chemistry, 163, 1-9, 10.1016/j.marchem.2014.03.007, 2014.

510 Butler, A.: Marine siderophores and microbial iron mobilization, Biometals, 18, 369-374, 10.1007/s10534-005-3711-0 2005.

Croot, P. L., Andersson, K., Öztürk, M., and Turner, D. R.: The distribution and speciation of iron along 6°E in the Southern Ocean, Deep Sea Research Part II: Topical Studies in Oceanography, 51, 2857-2879, 10.1016/j.dsr2.2003.10.012, 2004.

515 de Baar, H. J.: On iron limitation of the Southern Ocean : experimental observations in the Weddell and Scotia Seas, Marine Ecol. Prog. Ser., 65, 105-122, 10.3354/meps065105, 1990.

de Baar, H. J., Boyd, P. W., Coale, K. H., Landry, M. R., Tsuda, A., Assmy, P., Bakker, D. C., Bozec, Y., Barber, R. T., and Brzezinski, M. A.: Synthesis of iron fertilization experiments: from the iron age in the age of enlightenment, Journal of Geophysical Research: Oceans, 110, 10.1029/2004JC002601, 2005.

520 De Jong, J. T. M., Stammerjohn, S. E., Ackley, S. F., Tison, J. L., Mattielli, N., and Schoemann, V.: Sources and fluxes of dissolved iron in the Bellingshausen Sea (West Antarctica): The importance of sea ice, icebergs and the continental margin, Marine Chemistry, 177, 518-535, 10.1016/j.marchem.2015.08.004, 2015.

De La Rocha, C.: 8.4 - The Biological Pump, in: The oceans and marine geochemistry, second ed., Elsevier, Oxford, 83, 2006.

525 Genovese, C., Grotti, M., Pittaluga, J., Ardini, F., Janssens, J., Wuttig, K., Moreau, S., and Lannuzel, D.: Influence of organic complexation on dissolved iron distribution in East Antarctic pack ice, Marine Chemistry, 203, 28-37, 10.1016/j.marchem.2018.04.005, 2018.

Gerringa, L., Laan, P., Arrigo, K., van Dijken, G., and Alderkamp, A.-C.: The organic complexation of iron in the Ross sea, Marine Chemistry, 103672, 10.1016/j.marchem.2019.103672, 2019.

530 Gerringa, L. J., Rijkenberg, M. J., Thuróczy, C.-E., and Maas, L. R.: A critical look at the calculation of the binding characteristics and concentration of iron complexing ligands in seawater with suggested improvements, Environmental Chemistry, 11, 114-136, 10.1071/EN13072, 2014.

Gerringa, L. J. A., Blain, S., Laan, P., Sarthou, G., Veldhuis, M. J. W., Brussaard, C. P. D., Viollier, E., and Timmermans, K. R.: Fe-binding dissolved organic ligands near the Kerguelen Archipelago in the

535 Southern Ocean (Indian sector), Deep Sea Research Part II: Topical Studies in Oceanography, 55, 606-621, 10.1016/j.dsr2.2007.12.007, 2008.

Gerringa, L. J. A., Rijkenberg, M. J. A., Schoemann, V., Laan, P., and de Baar, H. J. W.: Organic complexation of iron in the West Atlantic Ocean, Marine Chemistry, 177, 434-446, 10.1016/j.marchem.2015.04.007, 2015.

540 Gledhill, M., and Buck, K.: The organic complexation of iron in the marine environment: A review, Frontiers in Microbiology, 3, 10.3389/fmicb.2012.00069, 2012.

Gledhill, M., and Gerringa, L. J. A.: The Effect of Metal Concentration on the Parameters Derived from Complexometric Titrations of Trace Elements in Seawater—A Model Study, Frontiers in Marine Science, 4, 10.3389/fmars.2017.00254, 2017.

545 Grotov, A. S., Nechaev, D. A., Panteleev, G. G., and Yaremchuk, M. I.: Large scale circulation in the Bellingshausen and Amundsen seas as a variational inverse of climatological data, Journal of Geophysical Research: Oceans, 103, 13011-13022, 10.1029/98jc00449, 1998.

Hassler, C., Cabanes, D., Blanco-Ameijeiras, S., Sander, S. G., and Benner, R.: Importance of refractory ligands and their photodegradation for iron oceanic inventories and cycling, Marine and Freshwater Research,

550 71, 311-320, 10.1071/MF19213, 2020.

Hassler, C. S., van den Berg, C. M. G., and Boyd, P. W.: Toward a Regional Classification to Provide a More Inclusive Examination of the Ocean Biogeochemistry of Iron-Binding Ligands, Frontiers in Marine Science, 4, 10.3389/fmars.2017.00019, 2017.

Henley, S. F., Schofield, O. M., Hendry, K. R., Schloss, I. R., Steinberg, D. K., Moffat, C., Peck, L. S., Costa, D.

555 P., Bakker, D. C. E., Hughes, C., Rozema, P. D., Ducklow, H. W., Abele, D., Stefels, J., Van Leeuwe, M. A., Brussaard, C. P. D., Buma, A. G. J., Kohut, J., Sahade, R., Friedlaender, A. S., Stammerjohn, S. E., Venables, H. J., and Meredith, M. P.: Variability and change in the west Antarctic Peninsula marine system: Research priorities and opportunities, Progress in Oceanography, 173, 208-237, 10.1016/j.pocean.2019.03.003, 2019.

560 Hofmann, E. E., and Klinck, J. M.: Thermohaline variability of the waters overlying the west Antarctic Peninsula continental shelf, Ocean, Ice, and Atmosphere: Interactions at the Antarctic Continental Margin, Antarct. Res. Ser, 75, 67-81, 10.1029/AR075p0067, 1998.

Joy-Warren, H. L., van Dijken, G. L., Alderkamp, A.-C., Leventer, A., Lewis, K. M., Selz, V., Lowry, K. E., van de Poll, W., and Arrigo, K. R.: Light Is the Primary Driver of Early Season Phytoplankton Production

565 Along the Western Antarctic Peninsula, Journal of Geophysical Research: Oceans, 124, 7375-7399, 10.1029/2019jc015295, 2019.

Klinck, J. M., Hofmann, E. E., Beardsley, R. C., Salihoglu, B., and Howard, S.: Water-mass properties and circulation on the west Antarctic Peninsula Continental Shelf in Austral Fall and Winter 2001, Deep Sea Research Part II: Topical Studies in Oceanography, 51, 1925-1946, 10.1016/j.dsr2.2004.08.001, 2004.

570 Klunder, M. B., Laan, P., Middag, R., De Baar, H. J. W., and van Ooijen, J. C.: Dissolved iron in the Southern Ocean (Atlantic sector), Deep Sea Research Part II: Topical Studies in Oceanography, 58, 2678-2694, 10.1016/j.dsr2.2010.10.042, 2011.

Krachler, R., Krachler, R. F., Wallner, G., Hann, S., Laux, M., Cervantes Recalde, M. F., Jirsa, F., Neubauer, E., von der Kammer, F., Hofmann, T., and Keppler, B. K.: River-derived humic substances as iron chelators in seawater, Marine Chemistry, 174, 85-93, 10.1016/j.marchem.2015.05.009, 2015.

Kuma, K., Nishioka, J., and Matsunaga, K.: Controls on iron(III) hydroxide solubility in seawater: The influence of pH and natural organic chelators, Limnology and Oceanography, 41, 396-407, 10.4319/lo.1996.41.3.0396, 1996.

Laglera, L. M., Sukekava, C. F., Slagter, H. A., Downes, J., Aparicio-Gonzalez, A., and Gerringa, L. J.: First Quantification of the Controlling Role of Humic Substances in the Transport of Iron Across the Surface of the Arctic Ocean, Environmental science & technology, 53, 13136-13145, 10.1021/acs.est.9b04240, 2019a.

Laglera, L. M., Tovar-Sanchez, A., Sukekava, C. F., Naik, H., Naqvi, S. W. A., and Wolf-Gladrow, D. A.: Iron organic speciation during the LOHAFEX experiment: Iron ligands release under biomass control by copepod grazing, Journal of Marine Systems, 103151, 10.1016/j.jmarsys.2019.02.002, 2019b.

Lam, P. J., Doney, S. C., and Bishop, J. K. B.: The dynamic ocean biological pump: Insights from a global compilation of particulate organic carbon, CaCO3, and opal concentration profiles from the mesopelagic, Global Biogeochemical Cycles, 25, 10.1029/2010gb003868, 2011.

Lannuzel, D., Grotti, M., Abelmoschi, M. L., and van der Merwe, P.: Organic ligands control the concentrations of dissolved iron in Antarctic sea ice, Marine Chemistry, 174, 120-130, 10.1016/j.marchem.2015.05.005, 2015.

Lannuzel, D., Vancoppenolle, M., van der Merwe, P., de Jong, J. T. M., Meiners, K. M., Grotti, M., Nishioka, J., and Schoemann, V.: Iron in sea ice: Review and new insights, Elem. Sci. Anth., 4, 10.12952/journal.elementa.000130, 2016.

Lauderdale, J. M., Braakman, R., Forget, G., Dutkiewicz, S., and Follows, M. J.: Microbial feedbacks optimize ocean iron availability, Proceedings of the National Academy of Sciences, 117, 4842-4849, 10.1073/pnas.1917277117, 2020.

Le Quéré, C., Andrew, R. M., Canadell, J. G., Sitch, S., Korsbakken, J. I., Peters, G. P., Manning, A. C., Boden, T. A., Tans, P. P., Houghton, R. A., Keeling, R. F., Alin, S., Andrews, O. D., Anthoni, P., Barbero, L., Bopp, L., Chevallier, F., Chini, L. P., Ciais, P., Currie, K., Delire, C., Doney, S. C., Friedlingstein, P., Gkritzalis, T., Harris, I., Hauck, J., Haverd, V., Hoppema, M., Klein Goldewijk, K., Jain, A. K., Kato, E., Körtzinger, A., Landschützer, P., Lefèvre, N., Lenton, A., Lienert, S., Lombardozzi, D., Melton, J. R., Metzl, N., Millero, F., Monteiro, P. M. S., Munro, D. R., Nabel, J. E. M. S., Nakaoka, S., O'Brien, K., Olsen, A., Omar, A. M., Ono, T., Pierrot, D., Poulter, B., Rödenbeck, C., Salisbury, J., Schuster, U., Schwinger, J., Séférian, R., Skjelvan, I., Stocker, B. D., Sutton, A. J., Takahashi, T., Tian, H., Tilbrook, B., van der Laan-Luijkx, I. T., van der Werf, G. R., Viovy, N., Walker, A. P., Wiltshire, A. J., and Zaehle, S.: Global Carbon Budget 2016, Earth Syst. Sci. Data, 8, 605-649, 10.5194/essd-8-605-2016, 2016.

Lin, H., and Twining, B. S.: Chemical speciation of iron in Antarctic waters surrounding free-drifting icebergs, Marine Chemistry, 128-129, 81-91, 10.1016/j.marchem.2011.10.005, 2012.

Liu, X., and Millero, F. J.: The solubility of iron hydroxide in sodium chloride solutions, Geochimica et Cosmochimica Acta, 63, 3487-3497, 10.1016/S0016-7037(99)00270-7, 1999.

Liu, X., and Millero, F. J.: The solubility of iron in seawater, Marine Chemistry, 77, 43-54, 10.1016/S0304-4203(01)00074-3, 2002.

Macrellis, H. M., Trick, C. G., Rue, E. L., Smith, G., and Bruland, K. W.: Collection and detection of natural iron-binding ligands from seawater, Marine Chemistry, 76, 175-187, 2001.

Maldonado, M. T., Strzepek, R. F., Sander, S., and Boyd, P. W.: Acquisition of iron bound to strong organic complexes, with different Fe binding groups and photochemical reactivities, by plankton communities

in Fe-limited subantarctic waters, Global Biogeochemical Cycles, 19, doi:10.1029/2005GB002481, 2005.

620   Martin, J. H., Gordon, M., and Fitzwater, S. E.: The case for iron, 36, 1793-1802, doi:10.4319/lo.1991.36.8.1793, 1991.

Mawji, E., Gledhill, M., Milton, J. A., Tarran, G. A., Ussher, S., Thompson, A., Wolff, G. A., Worsfold, P. J., and Achterberg, E. P.: Hydroxamate Siderophores: Occurrence and Importance in the Atlantic Ocean, Environmental Science & Technology, 42, 8675-8680, 10.1021/es801884r, 2008.

625   Middag, R., De Baar, H., Laan, P., and Bakker, K.: Dissolved aluminium and the silicon cycle in the Arctic Ocean, Marine Chemistry, 115, 176-195, 10.1016/j.marchem.2009.08.002, 2009.

Middag, R., de Baar, H. J. W., Klunder, M. B., and Laan, P.: Fluxes of dissolved aluminum and manganese to the Weddell Sea and indications for manganese co-limitation, Limnology and Oceanography, 58, 287-300, 10.4319/lo.2013.58.1.0287, 2013.

630   Middag, R., de Baar, H. J. W., Bruland, K. W., and van Heuven, S. M. A. C.: The Distribution of Nickel in the West-Atlantic Ocean, Its Relationship With Phosphate and a Comparison to Cadmium and Zinc, Frontiers in Marine Science, 7, 10.3389/fmars.2020.00105, 2020.

Mikaloff Fletcher, S., Gruber, N., Jacobson, A. R., Doney, S., Dutkiewicz, S., Gerber, M., Follows, M., Joos, F., Lindsay, K., and Menemenlis, D.: Inverse estimates of anthropogenic CO2 uptake, transport, and storage
635   by the ocean, Global biogeochemical cycles, 20, 10.1029/2005GB002530, 2006.

Moffat, C., and Meredith, M.: Shelf-ocean exchange and hydrography west of the Antarctic Peninsula: a review, Philosophical Transactions of the Royal Society A: Mathematical, Physical and Engineering Sciences, 376, 20170164, 10.1098/rsta.2017.0164, 2018.

Moore, C. M., Mills, M. M., Arrigo, K. R., Berman-Frank, I., Bopp, L., Boyd, P. W., Galbraith, E. D., Geider, R.
640   J., Guieu, C., Jaccard, S. L., Jickells, T. D., La Roche, J., Lenton, T. M., Mahowald, N. M., Maranon, E., Marinov, I., Moore, J. K., Nakatsuka, T., Oschlies, A., Saito, M. A., Thingstad, T. F., Tsuda, A., and Ulloa, O.: Processes and patterns of oceanic nutrient limitation, Nature Geosci, 6, 701-710, 10.1038/ngeo1765, 2013.

Mopper, K., Kieber, D. J., and Stubbins, A.: Chapter 8 - Marine Photochemistry of Organic Matter: Processes and
645   Impacts, in: Biogeochemistry of Marine Dissolved Organic Matter (Second Edition), edited by: Hansell, D. A., and Carlson, C. A., Academic Press, Boston, 389-450, 2015.

Nolting, R. F., Gerringa, L. J. A., Swagerman, M. J. W., Timmermans, K. R., and de Baar, H. J. W.: Fe (III) speciation in the high nutrient, low chlorophyll Pacific region of the Southern Ocean, Marine Chemistry, 62, 335-352, 10.1016/S0304-4203(98)00046-2, 1998.

650   Norman, L., Thomas, D. N., Stedmon, C. A., Granskog, M. A., Papadimitriou, S., Krapp, R. H., Meiners, K. M., Lannuzel, D., van der Merwe, P., and Dieckmann, G. S.: The characteristics of dissolved organic matter (DOM) and chromophoric dissolved organic matter (CDOM) in Antarctic sea ice, Deep Sea Research Part II: Topical Studies in Oceanography, 58, 1075-1091, 10.1016/j.dsr2.2010.10.030, 2011.

Norman, L., Worms, I. A. M., Angles, E., Bowie, A. R., Nichols, C. M., Ninh Pham, A., Slaveykova, V. I.,
655   Townsend, A. T., David Waite, T., and Hassler, C. S.: The role of bacterial and algal exopolymeric substances in iron chemistry, Marine Chemistry, 173, 148-161, 10.1016/j.marchem.2015.03.015, 2015.

Orsi, A. H., Whitworth, T., and Nowlin, W. D.: On the meridional extent and fronts of the Antarctic Circumpolar Current, Deep Sea Research Part I: Oceanographic Research Papers, 42, 641-673, 10.1016/0967-0637(95)00021-W, 1995.

660   Poorvin, L., Sander, S. G., Velasquez, I., Ibisanmi, E., LeCleir, G. R., and Wilhelm, S. W.: A comparison of Fe bioavailability and binding of a catecholate siderophore with virus-mediated lysates from the marine bacterium Vibrio alginolyticus PWH3a, Journal of Experimental Marine Biology and Ecology, 399, 43-47, 10.1016/j.jembe.2011.01.016, 2011.

Powell, R. T., and Wilson-Finelli, A.: Photochemical degradation of organic iron complexing ligands in seawater, Aquatic Sciences, 65, 367-374, 10.1007/s00027-003-0679-0, 2003.

Raven, J. A., and Falkowski, P. G.: Oceanic sinks for atmospheric CO2, Plant, Cell & Environment, 22, 741-755, 10.1046/j.1365-3040.1999.00419.x, 1999.

Rijkenberg, M. J., Gerringa, L. J., Timmermans, K. R., Fischer, A. C., Kroon, K. J., Buma, A. G., Wolterbeek, B. T., and de Baar, H. J.: Enhancement of the reactive iron pool by marine diatoms, Marine Chemistry, 109, 29-44, 10.1016/j.marchem.2007.12.001, 2008.

Saito, M., Goepfert, T., Noble, A., Bertrand, E., Sedwick, P. N., and DiTullio, G. R.: A Seasonal Study of Dissolved Cobalt in the Ross Sea, Antarctica: Micronutrient Behavior, Absence of Scavenging, and Relationships with Zd, Cd, and P, Biogeosciences, 7, 10.5194/bgd-7-6387-2010, 2010.

Saito, M. A., and Goepfert, T. J.: Zinc-cobalt colimitation of Phaeocystis antarctica, Limnology and Oceanography, 53, 266-275, 10.4319/lo.2008.53.1.0266, 2008.

Sato, M., Takeda, S., and Furuya, K.: Iron regeneration and organic iron(III)-binding ligand production during in situ zooplankton grazing experiment, Marine Chemistry, 106, 471-488, 10.1016/j.marchem.2007.05.001, 2007.

Schoffman, H., Lis, H., Shaked, Y., and Keren, N.: Iron–Nutrient Interactions within Phytoplankton, Frontiers in Plant Science, 7, 10.3389/fpls.2016.01223, 2016.

Schofield, O., Saba, G., Coleman, K., Carvalho, F., Couto, N., Ducklow, H., Finkel, Z., Irwin, A., Kahl, A., Miles, T., Montes-Hugo, M., Stammerjohn, S., and Waite, N.: Decadal variability in coastal phytoplankton community composition in a changing West Antarctic Peninsula, Deep Sea Research Part I: Oceanographic Research Papers, 124, 42-54, 10.1016/j.dsr.2017.04.014, 2017.

Seyitmuhammedov, K., Stirling, C. H., Reid, M. R., van Hale, R., Laan, P., Arrigo, K. R., van Dijken, G., Alderkamp, A.-C., and Middag, R.: The distribution of Fe across the shelf of the Western Antarctic Peninsula at the start of the phytoplankton growing season, Marine Chemistry, in review.

Sherrell, R. M., Annett, A. L., Fitzsimmons, J. N., Roccanova, V. J., and Meredith, M. P.: A shallow bathtub ring of local sedimentary iron input maintains the Palmer Deep biological hotspot on the West Antarctic Peninsula shelf, Philosophical Transactions of the Royal Society A: Mathematical, Physical and Engineering Sciences, 376, 20170171, 10.1098/rsta.2017.0171, 2018.

Slagter, H. A., Gerringa, L. J. A., and Brussaard, C. P. D.: Phytoplankton Virus Production Negatively Affected by Iron Limitation, Frontiers in Marine Science, 3, 156 10.3389/fmars.2016.00156, 2016.

Slagter, H. A., Reader, H. E., Rijkenberg, M. J. A., Rutgers van der Loeff, M., de Baar, H. J. W., and Gerringa, L. J. A.: Organic Fe speciation in the Eurasian Basins of the Arctic Ocean and its relation to terrestrial DOM, Marine Chemistry, 197, 11-25, 10.1016/j.marchem.2017.10.005, 2017.

Smith, D. A., Hofmann, E. E., Klinck, J. M., and Lascara, C. M.: Hydrography and circulation of the West Antarctic Peninsula Continental Shelf, Deep Sea Research Part I: Oceanographic Research Papers, 46, 925-949, 10.1016/S0967-0637(98)00103-4, 1999.

Stammerjohn, S., Massom, R., Rind, D., and Martinson, D.: Regions of rapid sea ice change: An inter-hemispheric seasonal comparison, Geophysical Research Letters, 39, 2012.

Sunda, W. G.: Trace metal interactions with marine phytoplankton, Biological Oceanography, 6, 411-442, 10.1080/01965581.1988.10749543, 1989.

Takeda, S.: Influence of iron availability on nutrient consumption ratio of diatoms in oceanic waters, Nature, 393, 774-777, 10.1038/31674, 1998.

Thuróczy, C.-E., Alderkamp, A.-C., Laan, P., Gerringa, L. J. A., Mills, M. M., Van Dijken, G. L., De Baar, H. J. W., and Arrigo, K. R.: Key role of organic complexation of iron in sustaining phytoplankton blooms in the Pine Island and Amundsen Polynyas (Southern Ocean), Deep Sea Research Part II: Topical Studies in Oceanography, 71-76, 49-60, 10.1016/j.dsr2.2012.03.009, 2012.

710 Thuróczy, C. E., Gerringa, L. J. A., Klunder, M. B., Laan, P., and de Baar, H. J. W.: Observation of consistent trends in the organic complexation of dissolved iron in the Atlantic sector of the Southern Ocean, Deep Sea Research Part II: Topical Studies in Oceanography, 58, 2695-2706, 10.1016/j.dsr2.2011.01.002, 2011.

Tomczak, M., and Godfrey, J.: Regional oceanography: An introduction, Daya, New Delhi, 10.1016/C2009-0-
715 14825-0, 2003.

Turner, J., Maksym, T., Phillips, T., Marshall, G. J., and Meredith, M. P.: The impact of changes in sea ice advance on the large winter warming on the western Antarctic Peninsula, International Journal of Climatology, 33, 852-861, 10.1002/joc.3474, 2013.

Turner, J., Marshall, G. J., Clem, K., Colwell, S., Phillips, T., and Lu, H.: Antarctic temperature variability and
720 change from station data, International Journal of Climatology, 40, 2986-3007, 10.1002/joc.6378, 2020.

Twining, B. S., Baines, S. B., and Fisher, N. S.: Element stoichiometries of individual plankton cells collected during the Southern Ocean Iron Experiment (SOFeX), Limnology and Oceanography, 49, 2115-2128, 10.4319/lo.2004.49.6.2115, 2004.

Velasquez, I., Nunn, B. L., Ibisanmi, E., Goodlett, D. R., Hunter, K. A., and Sander, S. G.: Detection of
725 hydroxamate siderophores in coastal and Sub-Antarctic waters off the South Eastern Coast of New Zealand, Marine Chemistry, 126, 97-107, 10.1016/j.marchem.2011.04.003, 2011.

Velasquez, I. B., Ibisanmi, E., Maas, E. W., Boyd, P. W., Nodder, S., and Sander, S. G.: Ferrioxamine siderophores detected amongst iron binding ligands produced during the remineralization of marine particles, Frontiers in Marine Science, 3, 172, 10.3389/fmars.2016.00172, 2016.

730 Viljoen, J. J., Philibert, R., Van Horsten, N., Mtshali, T., Roychoudhury, A. N., Thomalla, S., and Fietz, S.: Phytoplankton response in growth, photophysiology and community structure to iron and light in the Polar Frontal Zone and Antarctic waters, Deep Sea Research Part I: Oceanographic Research Papers, 141, 118-129, 10.1016/j.dsr.2018.09.006, 2018.

Whitby, H., Planquette, H., Cassar, N., Bucciarelli, E., Osburn, C. L., Janssen, D. J., Cullen, J. T., González, A.
735 G., Völker, C., and Sarthou, G.: A call for refining the role of humic-like substances in the oceanic iron cycle, Scientific reports, 10, 6144-6144, 10.1038/s41598-020-62266-7, 2020.

Wu, M., McCain, J. S. P., Rowland, E., Middag, R., Sandgren, M., Allen, A. E., and Bertrand, E. M.: Manganese and iron deficiency in Southern Ocean Phaeocystis antarctica populations revealed through taxon-specific protein indicators, Nature communications, 10, 1-10, 10.1038/s41467-019-11426-z, 2019.

740 Ye, Y., Völker, C., and Gledhill, M.: Exploring the Iron-Binding Potential of the Ocean Using a Combined pH and DOC Parameterization, Global Biogeochemical Cycles, 34, e2019GB006425, 10.1029/2019GB006425, 2020.